A techno-economic assessment of bioethanol production from switchgrass through biomass gasification and syngas fermentation

Energy 274 (2023) 127318

Contents lists available at ScienceDirect

Energy

journal homepage: www.elsevier.com/locate/energy

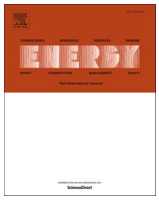

A techno-economic assessment of bioethanol production from switchgrass through biomass gasification and syngas fermentation

Francesco Regis [a,b], Alessandro Hugo Antonio Monteverde [a,*], Debora Fino [a,b]

[a] Department of Applied Science and Technology, Politecnico di Torino, Corso Duca degli Abruzzi 24, 10129, Turin, Italy
[b] Centre for Sustainable Future Technologies, Fondazione Istituto Italiano di Tecnologia, Via Livorno 60, 10144, Turin, Italy

ARTICLE INFO

Handling Editor: Petar Sabev Varbanov

Keywords:
Bioethanol
Gasification
Syngas fermentation
Techno-economic analysis
Process simulation
Aspen plus

ABSTRACT

The consumption of fossil fuels, which are not economically and environmentally sustainable, can be reduced by producing biofuels, such as bioethanol. This study presents a reproducible model of the ethanol production process developed with Aspen Plus® software. The work's goal is to enhance the amount of ethanol produced per tonne of biomass and, therefore, the carbon yield of the process. The main steps of the process are the gasification of the pretreated switchgrass, the cleaning of the syngas obtained, the fermentation of the syngas to ethanol and its purification. The parameters relating to gasification were set to produce syngas with an optimal composition for the fermenter. A discounted cash flow analysis was used to determine the minimum ethanol selling price for different plant scales and H_2 prices. By enriching the syngas with green H_2 and adopting an optimal bioreactor, a remarkable ethanol yield of 1015.04 L/t of switchgrass can be obtained. Considering a plant size of 750,000 t/y of switchgrass, the minimum ethanol selling price is 1.07 $/L for the base scenario and is further lowered to 0.77 $/L for the 2050 H_2 scenario. The potential savings of building more plants were also assessed thanks to the learning effects.

1. Introduction

According to the EIA, the global energy demand is expected to rise by 47% in the next 30 years and in the same time frame, the liquid fuel consumption is assumed to increase by 64% compared to 2020 levels [1]. This growth is due to the increase in the population and its per capita energy consumption. Fossil fuels cannot meet the ever-increasing demands because they are not economically and environmentally sustainable. The goal of the Paris Agreement, which entered into force in 2016, is to limit global warming to 1.5 K above pre-industrial levels. In a context where the time available is too short to eliminate the need for carbon-based fuels, the solution may be to increase the production of biofuels. While several types of resources, such as solar, wind, hydropower, and geothermal energy, can be utilized to produce energy and heat, biomass is the sole resource that can also produce chemicals and materials. In addition to fossil fuels, biomass is the sole carbon-rich resource on the planet [2]. Furthermore, the current political crisis in OPEC countries has a negative influence on the world's fossil-fuel-based energy sector [3]. In the United States in 2020 biofuels such as bioethanol and biodiesel contributed only 5% of the transport energy source, based on energy content, while fossil fuels accounted for 90% [4]. In the same year, the fraction of energy used for transport was 26% of the total in the United States [4]. From 2020 to 2025, the worldwide bioethanol market is expected to increase at a CAGR of 14.0% until reaching USD 64.8 billion [5]. Ethanol is found in more than 98% of gasoline sold in the United States, with E10 (10% ethanol, 90% gasoline) being the most common. Because ethanol has a high-octane number and a high oxygen content, the combustion of E10 is more complete than that of gasoline lowering air pollution.

To date, most ethanol is produced from food crops, such as corn and sugarcane, and is therefore classifiable as a first-generation biofuel. The disadvantages linked to the use of food crops are the food-fuel conflict, deforestation and the significant GHG emissions in the cultivation phases. The key to overcoming these challenges is to use second-generation materials such as forestry waste, agricultural residues or energy crops grown on marginal lands.

Commercial production of ethanol is divided between the biochemical and thermochemical routes. There are two main biochemical pathways. In the former the biomass is first hydrolysed with chemicals and enzymes and then fermented to make ethanol with microorganisms, such as yeast. In the second biochemical path occurs the enzymatic saccharification of the cellulose and the fermentation of the resulting glucose and xylose to ethanol. Instead, there are three main

* Corresponding author.
E-mail address: alessandro.monteverdevidela@polito.it (A.H.A. Monteverde).

https://doi.org/10.1016/j.energy.2023.127318
Received 16 September 2022; Received in revised form 20 March 2023; Accepted 23 March 2023
Available online 25 March 2023

Nomenclature

Acronyms and abbreviations

ABR	Air-to-Biomass Ratio
CAGR	Compound Annual Growth Rate
CHC	Chemocatalytic route
COD	Chemical Oxygen Demand
CSTR	Continuous-flow Stirred-Tank Reactor
EIA	United States Energy Information Administration
FTP	Fisher Tropsch Process
GCC	Gasification-Catalytic Conversion route
GF	Gasification-Fermentation route
GHG	Greenhouse Gases
HHV	Higher Heating Value
HX-Net	Aspen Energy Analyzer
IEC	Installed Cost of the Equipment
MESP	Minimum Ethanol Selling Price
NPV	Net Present Value
OPEC	Organization of the Petroleum Exporting Countries
PEC	Purchase Equipment Cost
PFD	Process Flow Diagram
PSA	Pressure Swing Adsorption
SBR	Steam-to-Biomass Ratio
SHF	Separate Hydrolysis-Fermentation route
SSF	Simultaneous Saccharification and Fermentation route
TCI	Total Capital Investment
TEC	Total Equipment Cost
TIC	Total Installed Cost
TPI	Total Project Investment
USD	United States Dollar
ΔT_{min}	Minimum Temperature Difference

Parameters

A	Equipment cost attribute
$CEPCI$	Chemical Engineering Plant Cost Index
DR	Discount Rate
IT	Income Taxes ($)
N_{EQ}	Number of nonparticulate processing step
N_{OS}	Number of operators per shift
p	Cost of the pioneer plant ($)
P_{SH}	Number of processing steps involving the handling of particulate solids
t	Time step (year)
TAS	Total Annual sale ($)
TPC	Total Production Costs ($)
x	Cumulative number of plants
y	Total project investment of the xth plant
α_1, α_2	Constant values for IEC calculations
γ	Cost exponent factor
η_C	Carbon yield of the process

Subscripts

1	Reference year
2	Base year
a	Required attribute
b	Base attribute

thermochemical pathways, two of which have in common the gasification of the biomass to produce synthesis gas (H_2, CO, CO_2) from which the impurities must be eliminated before proceeding to its transformation into ethanol. In the first route, the syngas is converted into ethanol over a catalyst, while in the second one microorganisms are exploited. Because of the Wood–Ljungdahl metabolic pathway, which allows them to produce acetate and ethanol as the main end products, acetogens are the most extensively used microorganism [6–8]. The last alternative is the chemocatalytic (CHC) route in which in a single step the biomass is transformed into ethanol and other by-products in a catalytic reactor.

The process route separate hydrolysis-fermentation (SHF) and simultaneous saccharification and fermentation (SSF) can only use the carbohydrates present in the feedstock as they are not able to convert the lignin which can account for up to 40% of the biomass [4]. Gasification, on the other hand, can convert all the biomass into syngas, thus guaranteeing high flexibility in the choice of feedstock. The conversion of syngas into ethanol is usually achieved by catalyst with the Fischer Tropsch Process (FTP), however, this route is less advantageous than using gas fermentation [9]. First of all, fermentation takes place at lower pressures and temperatures than FTP, thus allowing savings on both capital and operational costs. Secondly, the selectivity of the biological process is higher, so the by-products are less and the costs to purify the products are lower. Unlike syngas fermentation, FTP requires a fixed H_2:CO ratio, which usually is significantly higher than that obtained via biomass gasification. Finally, contrary to catalysts which are poisoned by the impurities present in the syngas, many bacteria are tolerant to low concentrations of some of them. This means that for the route gasification-fermentation (GF) the purification costs of the syngas are lower than those of the route gasification-catalytic conversion (GCC). The main obstacles to successful syngas fermentation are low ethanol yield, the resistance of microorganisms to syngas impurities, finding the optimum ethanol production conditions, bioreactor design, downstream processing and the integration at its best between gasification, syngas fermentation and ethanol purification.

Despite a growth in the number of papers on syngas fermentation, only a few have included simulations of the GF process [6–8,10–17]. Though these studies look at the entire process from feedstock to ethanol and provide useful estimates of process performance in technical and economic domains, the bioreactor simulations in some cases were based on strong assumptions, syngas and ethanol purifications were sometimes approximate, and the nutrients required by the bacteria inside the fermenters were never considered.

In this work, a system design for bioethanol production from switchgrass using gasification and syngas fermentation is proposed. The objectives are to increase the quantity of ethanol obtained per tonne of biomass and to calculate the related minimum ethanol selling price. The novelty lies in conceptualizing a process where the use of carbon obtains maximum values and in the detailed analysis of the units used for syngas and ethanol purifications. The gasification conditions were set to produce syngas with an H_2:CO ratio as close as possible to the optimal for the fermenter. To achieve the stoichiometric ratio between H_2 and CO, thus increasing ethanol production and decreasing carbon emissions, the syngas current was supplemented by a stream of green hydrogen. A section of the plant was dedicated to the removal of impurities produced during the gasification of biomass from syngas. The bioreactors were designed in a realistic way starting from pilot plant data. Other important issues addressed concern the consideration of the nutrients necessary for the bacteria both as regards their removal from ethanol and the costs per litre of medium.

Aspen Plus® was used to develop and simulate a process flowsheet ranging from switchgrass to ethanol. Additionally, a financial model was built to estimate the capital expenditure, the operating costs, and the minimum ethanol selling price through a discounted cash flow analysis.

2. Modelling

The process model was implemented on Aspen Plus® V10 software

(AspenTech, inc.). Thanks to the software it was possible to evaluate the different process units from reactor engineering to separation and finally refining. The energy integration was carried out using Aspen Energy Analyzer® V10 (AspenTech, inc.) software which made it possible to choose the most efficient integration of heat flows. To compute the physical properties of the materials, the Peng-Robinson equation of state with Boston Mathias modifications was used [17].

3. Process overview

The process chose to produce bioethanol consists of five main steps. Initially, the biomass was chopped and dried in the biomass pretreatment step, subsequently, in the gasification step the solid material was converted into syngas. Then, a purification step was necessary to remove potentially dangerous substances for bacteria during the fermentation phase. This purified gas was converted by selected microorganisms into ethanol, which was finally purified for sale. A simplified flow diagram of the overall process is presented in Fig. 1.

3.1. Section description

3.1.1. Biomass pretreatment

The biomass chosen to produce syngas was switchgrass. This herbaceous species was selected due to its high productivity, even in low quality lands and non-optimal climates [18]. The implementation of the switchgrass in the Aspen Plus® model and a list of all other components used in the simulation are reported, respectively, in Method S1 and Table S1 in the Supplementary Data.

The quantity of raw switchgrass processed annually by the plant was set at 1000 t. As can be seen from the process flow diagram (PFD) of the treatment section in Fig. 2, this raw biomass was first treated in a hammer mill (SR-101) and then dried (D-101) to reduce its humidity to a constant value. The mechanical equipment list of the PFD-A101 in Fig. 2 and all subsequent PFDs can be found in Table S2 in Supplementary Data.

The hammer mill (SR-101) was necessary to reduce the particle size of the biomass granting better flow properties and increasing the surface area. As a simplification the hammer mill (SR-101) was omitted from the Aspen Plus® model, therefore the composition of the currents 101 and 102 is the same. The need for utilities and the cost of the equipment neglected from the Aspen Plus® model were taken into consideration in the financial model. The following convective dryer (D-101), simulated as a Dryer block, has been set to obtain output switchgrass with 8 wt% moisture on a wet basis. The particle size distribution and the drying curve parameter of the biomass were taken, respectively, in Table 14.3 and Table 14.4 of J. Haydary book [19]. The stream table of all the currents of the PFD in Fig. 2 is reported in Table S3 in Supplementary Data.

3.1.2. Gasification

Downstream of the pre-treatment, the biomass was converted into syngas. To do this, there was a first decomposer reactor (R-201), in which the biomass was decomposed into components, and a second gasifier reactor (R-202). The PFD of the gasification section can be seen in Fig. 3, while the relating stream table is reported in Table S4 in Supplementary Data.

The parameters concerning the Aspen Plus® implementation of this equipment are given in Method S2 in the Supplementary Data.

The distribution between the various products leaving the gasifier was dependent on the temperature, the air-to-biomass ratio (ABR) and the steam-to-biomass ratio (SBR). The dimensionless quantities ABR and SBR are defined respectively in Eq. (1) and Eq. (2).

$$ABR = Air\ mass\ flow\ rate / Biomass\ mass\ flow\ rate \quad (1)$$

$$SBR = Steam\ mass\ flow\ rate / Biomass\ mass\ flow\ rate \quad (2)$$

Air and steam act as oxidizing agents. By varying the gasification temperature, ABR and SBR through sensitivity analysis it was possible to obtain the effects on the molar distribution of the output current from the gasifier. CO, H_2 and CO_2 were the components of greatest interest in syngas as regards the subsequent fermentation.

The trends of the molar fractions of the three components selected in stream 205, as the ABR, T and SBR vary, are shown respectively in Fig. S1, Fig. S2 and Fig. S3 in Supplementary Data. By keeping the gasification temperature and SBR fixed, as ABR increased the mole fraction of CO and H_2 decreased while that of CO_2 increased. Keeping ABR and SBR fixed, as the gasification temperature increased the mole fraction of CO and H_2 increased while that of CO_2 decreased. Finally, keeping T and ABR fixed, as SBR increased, the mole fraction of H_2 and CO_2 increased while that of CO decreased. The ideal molar composition of the syngas entering the first fermenter was given by about 38.8% of CO, 6.4% of CO_2 and 54.8% of H_2. Therefore, the ABR value was set equal to zero and the gasification temperature equal to 1173.15 K. In this way, the production of CO_2 in the gasifier was limited to the maximum rewarding that of CO and H_2. The gasification temperature was not raised above 1173.15 K to limit the effects of the Boudouard reaction and therefore the production of CO_2 and C obtained by converting the CO [20]. To identify the optimal SBR value, the molar composition of the purified syngas (stream 313 in Fig. 5) was analysed as this parameter varied. The trend of the molar fraction of CO, CO_2 and H_2 in the purified syngas, as the SBR varies, fixed ABR = 0 and T = 1173.15 K is presented in Fig. 4. At a value of SBR equal to 0.4 the composition of the purified syngas coincided with the optimal one for the first fermentation reactor, therefore this value was chosen.

Regarding the production of tar during gasification, it was conservatively assumed that these were 4 wt% of the switchgrass (current 103) [21]. To decrease the model complexity, the tar compounds group was

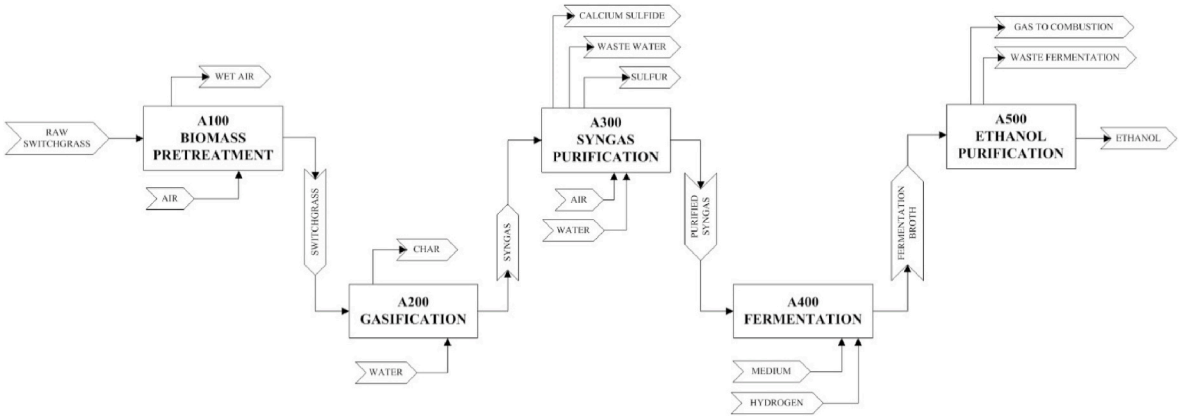

Fig. 1. General overview of the ethanol process structure.

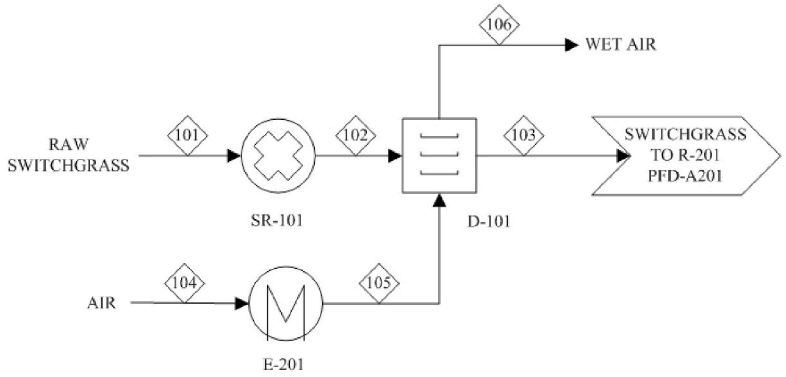

Fig. 2. PFD-A101 Biomass pretreatment.

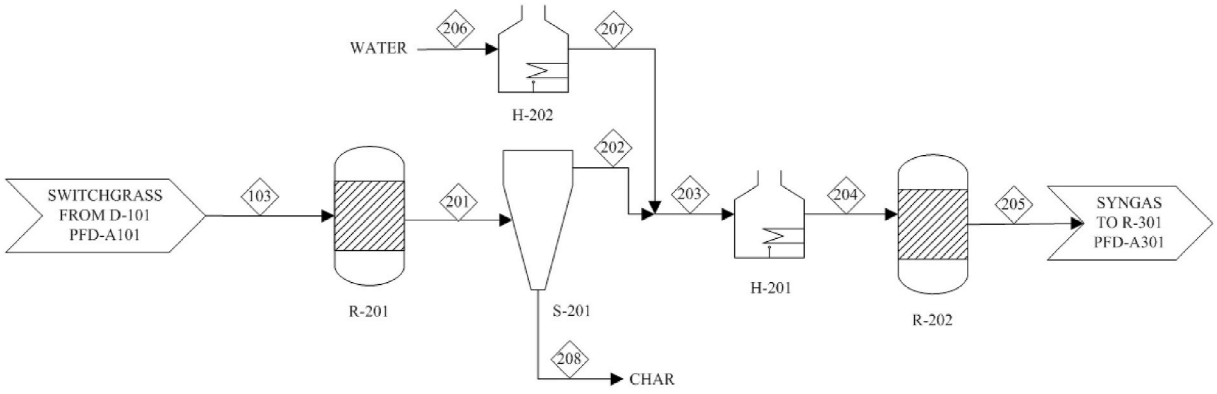

Fig. 3. PFD-A201 Gasification.

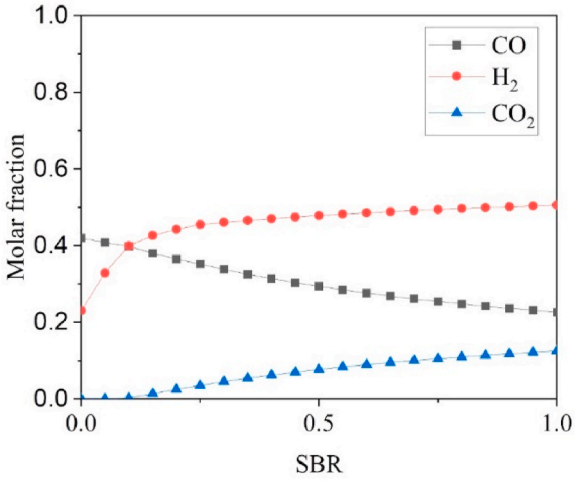

Fig. 4. Effect of steam-to-biomass ratio (SBR) on the molar distribution of the purified syngas (stream 313) at P = 1 atm, gasification temperature = 1173.15 K and ABR = 0. The target molar composition of the syngas to achieve was about 38.8% of CO, 6.4% of CO_2 and 54.8% of H_2.

represented by naphthalene which at 1173.15 K can be considered the major tar component [21].

In the plant engineering field, fluidized bed reactors are the best solution to gasify the biomass in case of scale-up [14]. In the fluidized bed reactor configuration there is no distinction between decomposer and gasifier, all reactions take place together.

3.1.3. Syngas Purification

Syngas is typically cleaned in several approaches [22–27]. The syngas must be cleaned before reaching the bacterial fermentation stage because the impurities could be harmful to the microorganism's growth, compromising their productivity [28]. The substances that were considered to be removed were CH_4, tar, COS, H_2S and NH_3. The PFD of the gasification section can be seen in Fig. 5, while the related stream table is reported in Table S7 in Supplementary Data.

For the cleaning of the syngas a dolomite bed reactor, a catalytic filter candle, a catalytic reactor to hydrolyze the carbonyl sulfide, two wet scrubbers and a LO-CAT process were used. The parameters concerning the Aspen Plus® implementation of this equipment are given in Method S3 in the Supplementary Data. At the end of the purification process the syngas complied with the specifications for fuel synthesis presented in Table 3.10 of Hanzon document [26].

3.1.4. Fermentation

For the fermentation of syngas, *Clostridium ljungdahlii* was chosen as the biocatalyst because it is one of the most studied and performing bacteria to produce ethanol from synthesis gas [29]. This anaerobic mesophilic bacteria has acetate and ethanol as primary metabolic by-products [29,30]. C. *ljungdahlii* behaves differently during syngas fermentation depending on the growth conditions and the presence of electron donors (CO_2 and H_2). Acidogenesis occurs when there is an abundance of nutrients, optimal pH and temperature, but a shortage of electron donors [31]. While in the case of nutrient scarcity, low temperature, low pH, and product inhibition, but an abundance of CO_2 and H_2, solventogenesis occurs [31]. During acidogenesis C. *ljunghdalii* mainly produces acetic acid, while during solventogenesis there is predominant production of ethanol with the conversion of the acetic acid produced during acidogenesis into the latter [31]. As tested by Richter et al. to optimize the parameters of the respective phases, two

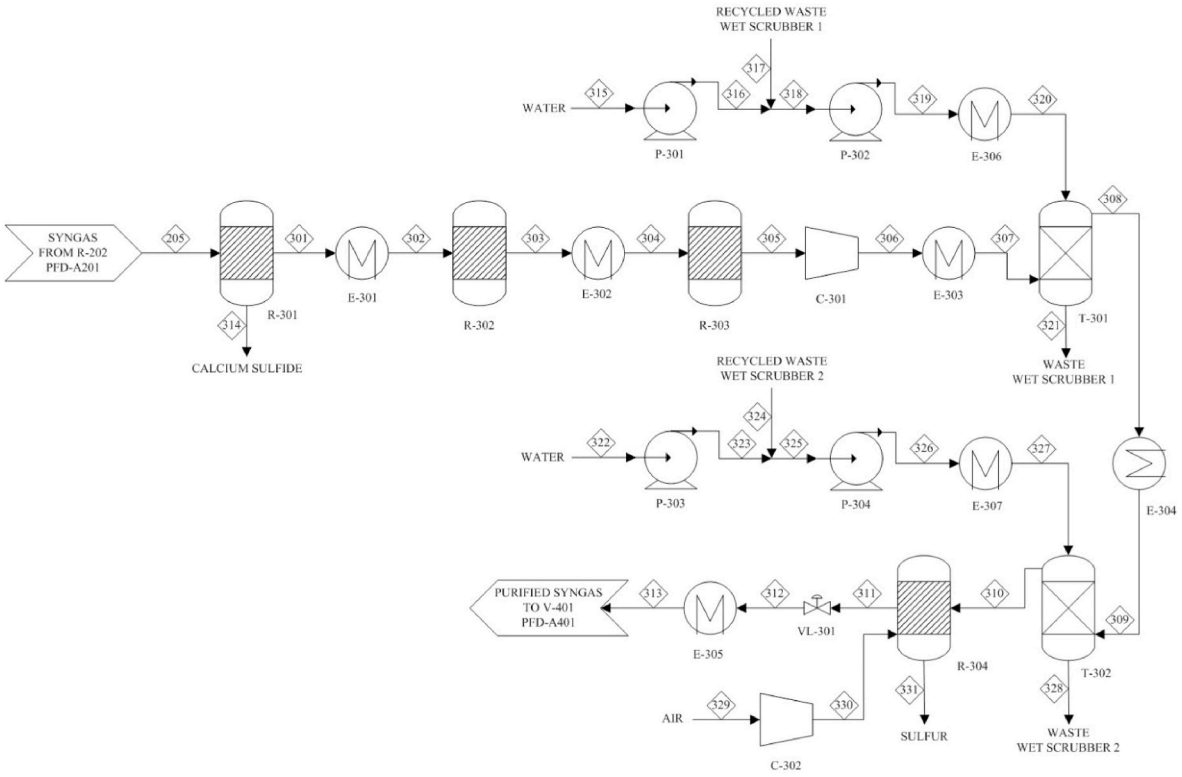

Fig. 5. PFD-A301 syngas purification.

fermentation reactors can be used: a first CSTR reactor in which the bacterium grows during acidogenesis and a second bubble column reactor in which solventogenesis takes place [31].

The PFD of the process chosen to ferment syngas to ethanol is presented in Fig. 6, while the relating stream table is reported in Table S8 in Supplementary Data.

The biochemical reactions that took place in the fermentation process can be simplified by the reactions presented in Eqs. (3)–(6) [32].

$$6CO + 3H_2O \rightarrow CH_3CH_2OH + 4CO_2 \quad (3)$$

$$2CO_2 + 6H_2 \rightarrow CH_3CH_2OH + 3H_2O \quad (4)$$

$$4CO + 2H_2O \rightarrow CH_3COOH + 2CO_2 \quad (5)$$

$$2CO_2 + 4H_2 \rightarrow CH_3COOH + 2H_2O \quad (6)$$

The Aspen Plus® modelling details of the fermentation section, including the fractional conversions of the reactions that occur in the reactors and the syngas divisions between them, are given in Method S4 in the Supplementary Data.

Among the inlet currents at the R-402 reactor, there was also one stream of green hydrogen (current 412) necessary to reach the stoichiometric ratio between H_2 and CO, thus increasing the production of ethanol and decreasing carbon emissions. Water and renewable electricity are used in the electrolysis process to produce green hydrogen. Under electricity input, water is separated into hydrogen and oxygen without carbon emissions [33]. Different electrolysis processes are currently utilized to produce hydrogen. The most well-known technologies include alkaline electrolysis cells, proton exchange membrane electrolysis cells and high-temperature solid oxide electrolysis cells [34]. Alkaline water electrolysis was chosen to produce green hydrogen because it is a well-established and relatively low cost technology [35].

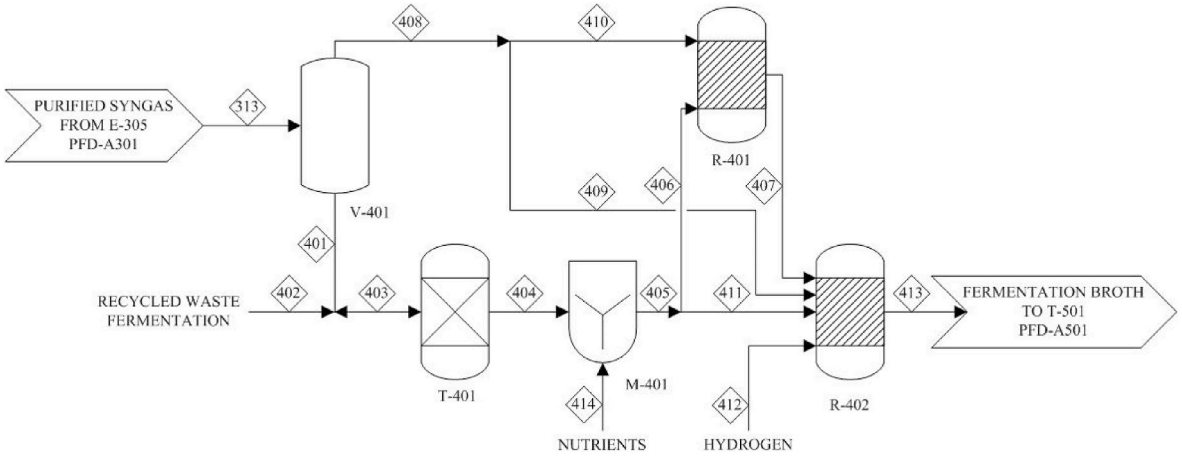

Fig. 6. PFD-A401 fermentation.

Gas recycling was used in both fermentation stages to optimize syngas residence time and mass transfer into the bacterial broth. However, rather than the mass transfer of the gas into the liquid phase, the productivity was restricted by the medium dilution rate (nutrient supply) under these conditions [31].

C. *ljungdahlii*, for simplification, was not included in the Aspen Plus® model. The biomass, however, would not have come out of the fermentation phase thanks to a 22 μm filter placed at the outlet of the R-401 reactor (current 413).

Other simplifications of the Aspen Plus® model concerned:

- the recycled waste fermentation current (402) that was just water, instead of the unpurged part of the waste fermentation current;
- the lack of the deionizer (T-401) and the nutrient mixer (M−401) which made the composition of the streams 403, 404 and 405 the same;
- the omission of nutrients (current 414) from the bacterial medium;
- the omission of the recirculation streams of the unconverted gas phase for the two reactors.

The need for utilities and the cost of the equipments omitted from the Aspen Plus® model were taken into consideration in the financial model. The list of nutrients necessary for C. *ljungdahlii* is given in Tables S11–S14 in Supplementary Data.

3.1.5. Ethanol purification

The fermentation broth needed to be purified to obtain commercial-grade ethanol. The PFD of the process chosen to purify the fermentation broth is presented in Fig. 7, while the related stream table is reported in Table S15 in Supplementary Data. For the purification of the ethanol were used ion exchange resins, flash drums, two distillation columns and a Pressure Swing Adsorption (PSA) process. The parameters concerning the Aspen Plus® implementation of this equipment are given in Method S5 in the Supplementary Data.

Ethanol (current 511) was thus obtained with a purity higher than 98.5 wt% together with 1.1 wt% of acetic acid and 0.4 wt% of water. With a switchgrass rate of 1000 t/y and an online time of 8760 h/y, the ethanol production rate was 1015035 L/y. The ethanol yield, defined as the ratio between the litre of ethanol produced per year and the tonne of biomass processed per year, was 1015.04 L/t of switchgrass. The waste fermentation (current 517) was mainly given by water, therefore the part of it recirculated, after being deionized (T-401), can be considered reusable by the process reducing the need for fresh water and the disposal costs. The gases obtained from the flashes and the first distillation column (current 522) were mainly a mixture of methane and nitrogen which were sent to combustion in the furnaces to limit environmental pollution.

3.2. Heat integration

To obtain the optimal design of the heat exchanger network that maximizes energy efficiency, the Aspen Energy Analyzer (HX-Net) software was used. HX-Net exploits pinch analysis to minimize the use of utilities. The pinch point is the point at which the distance between the hot composite curve and the cold composite curve is minimum. The hot composite curve relates temperature and enthalpy for the heat streams to be removed from the currents to be cooled, while the cold composite curve does so for the heat streams to be supplied to the currents to be heated [36]. The utility requirements are minimized by avoiding [36]:

- heat transfer between currents having a temperature difference equal to or lower than the pinch temperature;
- the use of cold utilities to cool currents over the pinch;
- the use of hot utilities to heat currents under the pinch.

In all heat exchange processes the ΔT_{min}, which represents the minimum temperature difference between the hot and cold sides, was set to 283.15 K. The Grid Diagram, which shows how process streams and utility streams were matched between each other using heat exchangers, is reported in Fig. S4 in Supplementary Data.

4. Process economics

One of the goals of developing a process design and simulation model was to evaluate the market potential of ethanol obtained from biomass gasification and syngas fermentation. From the analysis of the total project investment, variable and fixed costs it was possible to apply a discounted cash flow analysis to determine the production cost of ethanol when the net present value of the project was zero.

4.1. Total project investment

Purchase equipment costs (PEC) can usually be found in the literature or manufacturer price quotes. The relationship given in Eq. (7) was used to scale each PEC according to its size when pricing was known for a different size (or capacity) than what was required [37]. In Eq. (7) *A* is

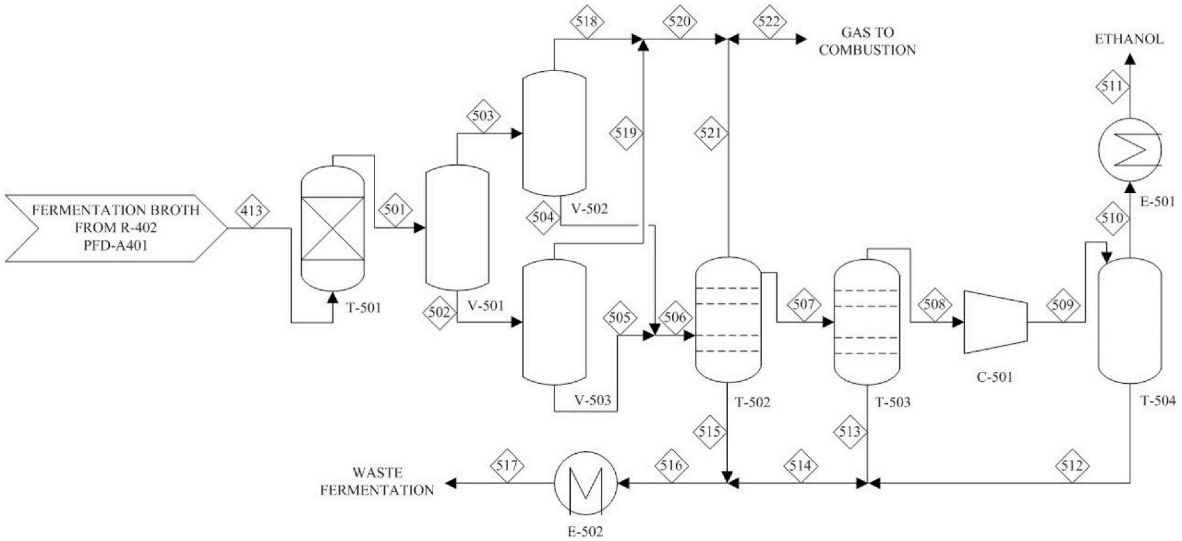

Fig. 7. PFD-A501 Ethanol purification.

the equipment cost attribute (size or capacity) and γ is a cost exponent factor depending on the equipment. In absence of other indications together with the quote, γ was considered equal to 0.6 for the six-tenths rule [37]. Subscripts a and b refer respectively to the equipment with the required and the base attribute.

$$PEC_a / PEC_b = (A_a/A_b)^{\gamma} \quad (7)$$

To scale all the PECs from the year for which they were available to 2021 which was chosen as the base year, Eq. (8) was used. In Eq. (8) *CEPCI* is the Chemical Engineering Plant Cost Index, while subscripts 1 and 2 refer respectively to the year when the cost is available and the base year [37].

$$PEC_1/PEC_2 = CEPCI_1/CEPCI_2 \quad (8)$$

The CEPCI, which takes into account the changes resulting from inflation, for 2021 was considered equal to 750.

The purchase costs of the various equipment are reported in Table S17 in the Supplementary Data. Fig. 8 shows the division of the equipment purchase costs between the different sections of the plant, keeping the heat exchange system separate.

To determine the installed cost of the equipment (IEC) was used Eq. (9).

$$IEC = PEC / (1 - \alpha_1 - \alpha_2) \quad (9)$$

in Eq. (9) α_1 is a constant equal to 0.24 which takes into account the labour necessary to install equipment, while α_2, which is equal to the value of 0.08, takes into account the costs of the materials necessary for the installation and of the building.

To obtain the total installed cost (TIC), the total capital investment (TCI) and the total project investment (TPI), other direct and indirect costs, presented in Table 1, must be added to the total equipment cost (TEC) [38]. TEC was obtained from the sum of all IEC. By adding the costs associated with warehouse and site development to the TEC, the TIC was derived. To obtain the TCI, the indirect costs (field expenses, home office, construction and project contingency) were added to the TIC. Finally, by adding to the TCI other start-up and commissioning costs, permits, fees and duties the TPI was obtained.

Table 1
Additional costs for determining the total project investment.

Item	Estimation	Cost in 2021 $
Total Equipment Cost (TEC)		**4337281**
Warehouse	1.5% of TEC	65059
Site Development	9.0% of TEC	390355
Total Installed Cost (TIC)		**4792696**
Field Expenses	20.0% of TIC	958539
Home Office & Construction Fee	25.0% of TIC	1198174
Project Contingency	3.0% of TIC	143781
Total Capital Investment (TCI)		**7093190**
Other Costs	10.0% of TIC	709319
Total Project Investment (TPI)		**7802509**

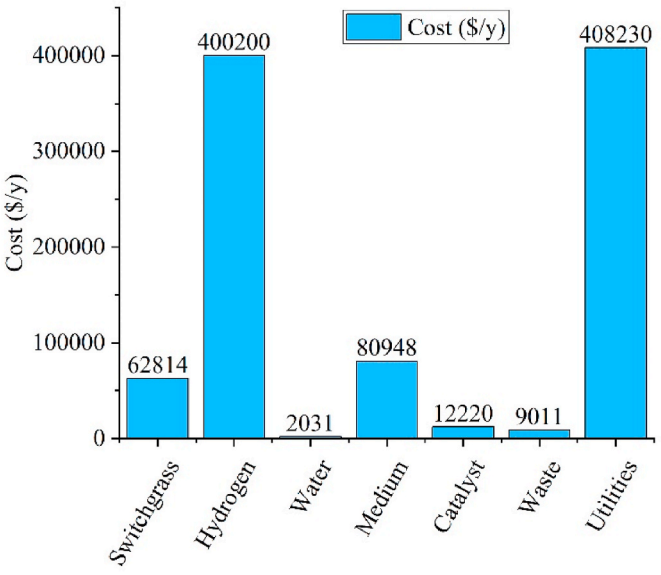

Fig. 9. Variable Operating Costs considering the conservative price of 6 $/kg for hydrogen.

4.2. Variable operating cost

Variable operating costs, which were considered only when the plant was in operation, included raw materials (switchgrass and hydrogen), water, medium, catalyst, waste handling and utilities. The annual distribution of these costs is shown in Fig. 9.

The cost considered for the switchgrass entering the plant was 62.81 $/t [39]. To keep the CO_2 footprint of the process as low as possible, it was chosen to use green hydrogen which was therefore produced with zero-carbon energy sources such as electrolysis powered by renewable electricity or aqueous phase reforming [40]. As specified in paragraph 3.1.4, the technology selected to produce green hydrogen was alkaline water electrolysis. The cost of green hydrogen varied between 2.5 and 6 $/kg, therefore the latter value was cautiously chosen [41]. The price of water for the required volumes was 1.1 $/m^3 [42]. The cost of nutrients necessary for bacterial growth was 0.0029 $/L medium [43]. The costs of the single nutrients per litre of the medium are reported in Table S18 in the Supplementary Data. Almost all of the costs related to the catalysts came from the Ni/Al_2O_3 (15 wt%) necessary for the catalytic filter candle (R-302) [44]. In the treatment of the waste were considered the purged fraction of the currents waste wet scrubber 1 (321), waste wet scrubber 2 (328) and waste fermentation (517), plus the disposal of the calcium sulfide (314). For streams 321, 328 and 517 was calculated the chemical oxygen demand (COD) and was considered a cost of 0.07 $/kg COD for the wastewater treatment [45]. For the waste treatment of stream 414, a price of 200 $/t was assumed [37]. The distribution of utilities costs in $/y is shown in Fig. 10. The cost of utilities was 74.5% due to power usage, which was calculated using ICARUS Process Evaluator, while the remaining 25.5% was due to heating and cooling and was calculated using Aspen Energy Analyzer®. The electric and thermal energy required in the production were, respectively, 3.87 kWh/L and 15.05 kWh/L of ethanol produced. Most of the electricity consumption is due to the hammer mill (SR-101) and the CSTR reactor (R-401).

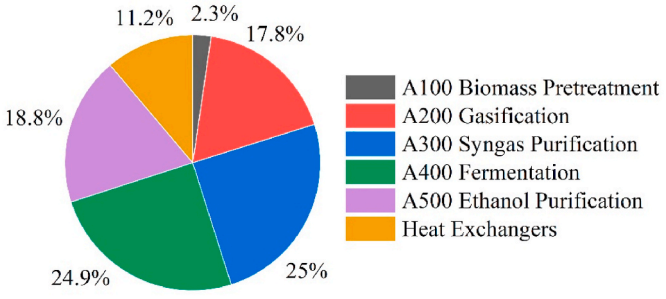

Fig. 8. Breakdown of the equipment cost between the different sections of the plant, keeping the heat exchange system separate.

4.3. Fixed operating cost

Whether the plant was working at full capacity or not, fixed operating costs were charged completely. Labour and several overhead elements were included in these costs. The technique used to estimate the

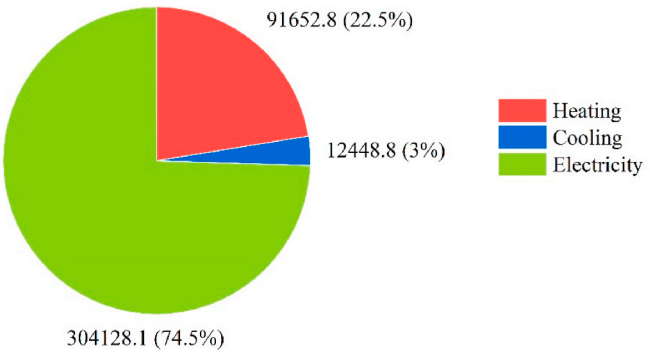

Fig. 10. Distribution of costs ($/y) among the various utilities.

salaries of the operational staff is given in Method S6 in the Supplementary Data.

To obtain the fixed operating costs must be added to the salaries the costs related to general overhead, maintenance, insurance and taxes, the estimate of which is presented in Table 2 [38].

4.4. Discounted cash flow analysis

A discounted cash flow rate of return analysis can be performed to establish the minimal selling price per litre of ethanol produced, once the total capital investment, variable operating expenses, and fixed operating costs were identified. The discounted cash flow analysis was done by iterating the ethanol selling cost until the project's net present value (NPV) was zero. The NPV can be calculated using Eq. (10) by subtracting the total plant investment (*TPI*) from the sum of discounted cash flows over the time horizon [46,47].

$$NPV = -TPI + \sum_{t=1}^{PL}(TAS - TPC - IT) \,/\, (1+DR)^t \tag{10}$$

The discounted cash flow was defined as the total annual sale (*TAS*) minus the total production costs (*TPC*) and the income taxes (*IT*). *DR* represents the discount rate, while the *t* index takes into account the years up to the plant life (*PL*). The necessary discounted cash flow analysis parameters, which are summed up in Table 3, were selected following the recommendations of Short et al. [48].

Regarding the depreciation system, the shortest was the recovery period the largest were the tax deductions. Due to fluctuations in the volume of ethanol produced and the depreciation deduction, the amount of income tax that must be paid varies year to year. Because depreciation deductions exceed net income in the early years of operation, no income tax is paid. Since the specific location of the plant had yet to be identified, state taxes were not taken into account. Unlike the construction time in which no income was earned, but the exits were many, the start-up period was not entirely lost. The discounted cash flow rate of return worksheet is reported in Table S19 in the Supplementary Data. With a switchgrass rate of 1000 t/y the ethanol production rate was 1015035 L/y which should be sold at MESP of 7.04 $/L. A summary worksheet of the ethanol production process economic analysis is reported in Table S20 in the Supplementary Data.

Table 2
Fixed operating costs.

Item	Estimation	Cost in 2021 $
Salaries		2885760
General overhead	60.0% of salaries	1731456
Maintenance	2.0% of TEC	86746
Insurance & Taxes	1.5% of TIC	71890
Fixed operating costs		**4775852.06**

Table 3
Discounted Cash Flow Analysis parameters.

Plant life	20 y
Discount rate	10%
General plant depreciation	200% declining balance
General plant recovery period	7 y
Federal tax rate	39%
Financing	100% equity
Construction period	2.5 y
First 6 months' expenditures	8%
Next 12 months' expenditures	60%
Last 12 months' expenditures	32%
Working capital	5% of TPI
Start-up time	0.5 y
Revenues during start-up	50% of normal
Variable cost during start-up	75% of normal
Fixed cost during start-up	100% of normal

5. Discussion

Applying the discounted cash flow analysis with the parameter reported in Table 3, plus total project investment, variable and fixed operating costs it was possible to determine the minimum ethanol selling price (MESP). With a switchgrass rate of 1000 t/y the ethanol should be sold at MESP of 7.04 $/L. The MESP was much higher than the ethanol market price which is around 0.4 $/L and reached a maximum of 0.92 $/L in 2013 [49]. The productivity range of corn bioethanol plants in the United States goes from 7 to 1420 ML/y with an average of 326 ML/y [50]. The bioethanol production of the modelled plant was only 1 ML/y starting from 1000 t/y of switchgrass. The effect of the plant size on the MESP was then investigated by scaling the plant to 15000, 40000, 70000, 100000, 300000, 500000, 750000, 1000000 and 1500000 t/y of switchgrass. To update the total project investment to the new sizes Eq. (7) was used, while the variable operating costs and the quantity of ethanol produced were scaled by proportion to the incoming biomass. The quantity of ethanol produced in the largest plant configuration (1500000 t/y) corresponded to an ethanol production equal to 1514 ML/y and therefore complies with the greater sizes reported in the literature.

From the graph in Fig. 11, it is possible to observe how MESP decreased as the size of the plant increased because the total project investment and fixed operating cost did not increase in proportion to the quantity of bioethanol produced. The most substantial reduction in the minimum ethanol selling price occurred in going from 1000 to 300000 t/y of switchgrass, with a decrease in the MESP from 7.04 to 1.12 $/L.

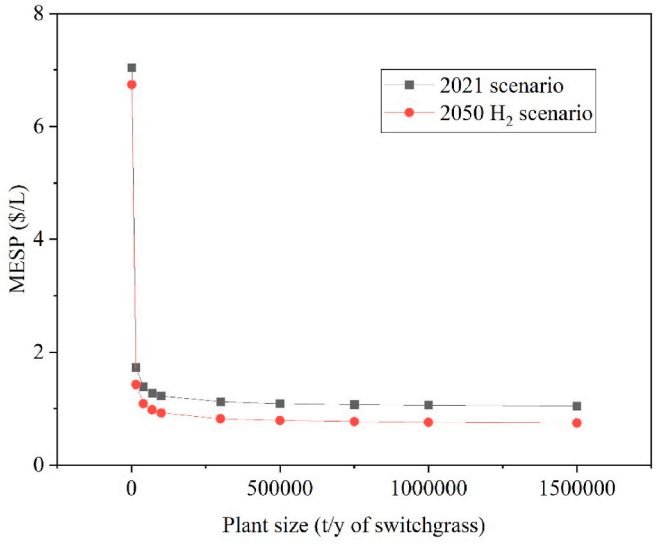

Fig. 11. Effect of plant size on minimum ethanol selling price (MESP).

Over 300,000 t/y of switchgrass, as the scale increased, the price decreased was minimal until reaching 1.05 $/L at 1,500,000 t/y of switchgrass. At a size of 300,000 t/y, there was an ethanol production of approximately 303 ML/y which corresponded to the most frequent size of corn bioethanol production plants in the United States [50]. As the size of the plant increased, the variable operating costs consequently increased, among which, as can be seen from Fig. 9, the most significant were linked to hydrogen and utilities. In the long-term (until 2050), scale-up and innovation could bring the cost of green hydrogen down to 1.5 $/kg [41]. As can be seen from Fig. 11, this would considerably lower the MESP. At a plant size of 300,000 t/y of switchgrass, the MESP would be 0.82 $/L, while for the largest plant size investigated it would be 0.75 $/L with a reduction of almost 30% compared to the case in which hydrogen was paid 6 $/kg. These latter costs were close to the market price of ethanol from fossil fuels. Furthermore, no credits or other incentives were considered in this analysis because of their variability with time, market location and starting feedstock. The minimum ethanol selling price with different plant sizes and hydrogen costs is reported in Table S21 in the Supplementary Data.

Biomass conversion and MESP were compared with techno-economic studies of bioethanol production from different routes reported in Table S22 in the Supplementary Data. The average plant size of the various analyses reported in Table S22 is about 750000 t/y of biomass, therefore the values are comparable with the corresponding plant size of our study. Considering the average of all the techno-economic studies presented, the MESP is 0.16 $/L, while the ethanol yield is 318.35 L/t. The MESP is lower than that found in this analysis as on average CHC, GCC, SSF and SHF allow for overall lower costs. On the other hand, the ethanol yield, of 1015.04 L/t of switchgrass, obtained from this analysis was about three times higher than that of all the mediated analyses and that of the single technologies, including those performed with the GF route. Such a high yield in this study is to be found in the enrichment of the syngas with H_2 to convert all the carbon present in the form of CO_2 and CO into ethanol, in the recirculation of the unconverted syngas inside the fermenters and in having used as a base for the scale-up of the fermenter a non-mass transfer limited process [31]. In particular, the carbon yield of the process, which can be calculated using Eq. (11), by adding hydrogen went from 49% to 72%.

$$\eta_C = mol\ C\ ethanol / mol\ C\ switchgrass \tag{11}$$

The advantages of the high yield in ethanol consist in the use of less biomass to produce the same quantity of ethanol, hence lower supply difficulties and transportation costs.

Finally, the average of the MESP of the only GF routes reported in Table S22 is 0.84 $/L. This value is comparable with the MESP values of this study at the same plant size which is 1.07 $/L for the base scenario and 0.77 $/L for the 2050 H_2 scenario.

From Table S22 it can be seen that for some studies the "*nth-plant*" economics assumption was adopted. In such cases, the researchers do not describe a pioneer plant; rather, numerous plants based on the same technology are already operating.

In the early stages of development, the cost of growing technology, such as biomass gasification or syngas fermentation, is typically relatively expensive. As more plants are established, the cost of the technologies falls and productivity rises because companies gather more experience. Eq. (12) can be used to represent this effect, which is referred to as a learning curve [51].

$$y = px^{-|\log(progress\ ratio)|/\log(2)} \tag{12}$$

in Eq. (12) y is the TPI of the xth plant, p is the cost of the pioneer plant and x is the cumulative number of plants. The progress ratio is defined in Eq. (13) [51].

$$progress\ ratio = 1 - learning\ rate \tag{13}$$

For the type of plant designed, a learning rate of 20% can be estimated and as a good benchmark can be considered the cost of constructing the tenth plant [51]. Fig. S5 in the Supplementary Data shows the learning curve effect on the pioneer Total Project Investment considering 750000 t/y of switchgrass as plant scale. From this graph, it is possible to see a 48% reduction in TPI at the tenth built plant. Therefore, considering the plant scale of 750,000 t/y and the 10-th plant built assumption the MESP for the base scenario was 1.02 $/L, while for the 2020$H_2$ scenario the MESP was reduced to 0.72 $/L.

As can be seen from Fig. 8, the section of the plant corresponding to the higher costs of the equipment was that of purification of the syngas. A recent study has shown that NH_3 and H_2S concentrations, respectively, of 4560 and 108 ppm inhibit the growth and product formation of C. *ljungdahlii* [52]. Concerning the other substances considered dangerous for the bacterium contained in the syngas, which were COS, CH_4 and tar, no concentration limit values were found. Also, for NH_3 and H_2S the inhibiting concentration was known, but not the maximum tolerated. This study considered the worst-case scenario and took as target values of the purification those necessary for the catalytic conversion of the syngas which are much more stringent than those for fermentation. These values were equal to or lower than 1 ppm therefore probably the purification of the syngas was oversized compared to the real needs [26]. Studies must be conducted to determine which are the allowed thresholds for syngas impurities that do not affect cell growth or product formation. A less severe purification of the syngas would ensure a lower MESP.

The large-scale project of two companies working together, Lanza-Tech Inc. and Aemetis, Inc., highlighted the potential of this second-generation biorefinery model. These two organizations set up a demonstration facility that gasifies waste orchard wood and almond and walnut shells to produce syngas then fermented to obtain commercial-grade ethanol [53]. The project was successful and Aemetis planned to build a commercial plant in California to produce 45 GL/y of bioethanol starting with 1.6 Mt/y of the same feedstocks [54].

6. Conclusions

This study investigated the process design and economics of converting biomass to ethanol through gasification and syngas fermentation from small to large scale. The process model was implemented on Aspen Plus® and all the data necessary to make the work reproducible were reported. Ethanol yield of 1015.04 L/t of switchgrass and MESP of 1.07 $/L were obtained in the basic case scenario, considering 750000 t/y of switchgrass processed. Even though the estimated ethanol selling prices were higher than the present ethanol market price, the results were comparable with those of other technologies for producing ethanol from a lignocellulosic matrix. On the other hand, an excellent yield of ethanol per tonne of biomass was obtained. Because of this high yield, less biomass is required to produce the same amount of ethanol, reducing supply issues and transportation costs. Thanks to the addition of green hydrogen to the syngas it was possible to increase the carbon yield of the process from 49 to 72%, also limiting C emissions. Surplus of electricity from renewable resources can be used to generate green hydrogen thanks to the electrolysis of water. In this way, otherwise wasted energy would be stored and low-cost hydrogen would be available for fermentation.

The ethanol production route via gasification-fermentation is highly adaptable because it allows any lignocellulosic biomass as well as waste to be used as feedstock. By adjusting the gasifier parameters to obtain the optimal syngas composition, the developed model may be applied to any feedstock.

Future improvements could be obtained from a better study of C. *ljungdahlii* and other non-acetogenic microorganisms. A lower MESP could be obtained thanks to higher concentrations of ethanol in the broth leaving the fermenter, using less expensive nutrients for the bacteria, changing the reactor configuration of the first fermentation reaction (R-401) as the impellers of the CSTR are energy demanding and

being more tolerant towards the impurities present in the syngas.

Biofuels are not to be intended only as final products, they can also be used as a starting base for other high-value chemicals. This is the case of butanol and butadiene which can be obtained from ethanol. Although the production of biofuels is growing rapidly, it is unlikely that they will be able to replace fossil fuels in a short period. However, the combination of biofuels and traditional pathways can limit the use of fossil fuels and greenhouse gas emissions.

Funding

This research did not receive any specific grant from funding agencies in the public, commercial, or not-for-profit sectors.

Credit author statement

Francesco Regis: Data curation; formal analysis; investigation; methodology; writing-review and editing. Alessandro Monteverde: conceptualization; supervision; writing-review and editing. Debora Fino: formal analysis and supervision.

Declaration of competing interest

The authors declare that they have no known competing financial interests or personal relationships that could have appeared to influence the work reported in this paper.

Data availability

Data will be made available on request.

Appendix B. Supplementary data

Supplementary data to this article can be found online at https://doi.org/10.1016/j.energy.2023.127318.

References

[1] Sun X, Atiyeh HK, Huhnke RL, Tanner RS. Syngas fermentation process development for production of biofuels and chemicals: a review. Bioresour Technol Reports 2019;7:100279. https://doi.org/10.1016/j.biteb.2019.100279.
[2] Panwar NL, Kaushik SC, Kothari S. Role of renewable energy sources in environmental protection: a review. Renew Sustain Energy Rev 2011;15:1513–24. https://doi.org/10.1016/j.rser.2010.11.037.
[3] Hossain MS, Theodoropoulos C, Yousuf A. Techno-economic evaluation of heat integrated second generation bioethanol and furfural coproduction. Biochem Eng J 2019;144:89–103. https://doi.org/10.1016/j.bej.2019.01.017.
[4] Liew FM, Martin ME, Tappel RC, Heijstra BD, Mihalcea C, Köpke M. Gas Fermentation-A flexible platform for commercial scale production of low-carbon-fuels and chemicals from waste and renewable feedstocks. Front Microbiol 2016;7. https://doi.org/10.3389/fmicb.2016.00694.
[5] Mizik T, Nagy L, Gabnai Z, Bai A. The major driving forces of the EU and US ethanol markets with special attention paid to the COVID-19 pandemic. Energies 2020;13:22. https://doi.org/10.3390/en13215614.
[6] Roy P, Dutta A, Deen B. Greenhouse gas emissions and production cost of ethanol produced from biosyngas fermentation process. Bioresour Technol 2015;192:185–91. https://doi.org/10.1016/j.biortech.2015.05.056.
[7] Michailos S, Parker D, Webb C. Design, sustainability analysis and multiobjective optimisation of ethanol production via syngas fermentation. Waste and Biomass Valorization 2019;10:865–76. https://doi.org/10.1007/s12649-017-0151-3.
[8] de Medeiros EM, Noorman H, Filho RM, Posada JA. Multi-objective sustainability optimization of biomass residues to ethanol via gasification and syngas fermentationtrade-offs between profitability, energy efficiency, and carbon emissions. Fermentation 2021;7. https://doi.org/10.3390/fermentation7040201.
[9] Ramachandriya K D, Kundiyana D K, Sharma A M, Kumar A, Atiyeh H K, Huhnke R L, et al. Critical factors affecting the integration of biomass gasification and syngas fermentation technology. AIMS Bioeng 2016;3:188–210. https://doi.org/10.3934/bioeng.2016.2.188.
[10] Safarian S, Unnthorsson R, Richter C. Simulation and performance analysis of integrated gasification-syngas fermentation plant for lignocellulosic ethanol production. Fermentation 2020;6. https://doi.org/10.3390/FERMENTATION6030068.
[11] Wagner H, Kaltschmitt M. Biochemical and thermochemical conversion of wood to ethanol—simulation and analysis of different processes. Biomass Convers Biorefinery 2013;3:87–102. https://doi.org/10.1007/s13399-012-0064-0.
[12] Piccolo C, Bezzo F. A techno-economic comparison between two technologies for bioethanol production from lignocellulose. Biomass Bioenergy 2009;33:478–91. https://doi.org/10.1016/j.biombioe.2008.08.008.
[13] Ardila YC, Figueroa JEJ, Lunelli BH, Filho RM, Maciel MRW. Simulation of ethanol production via fermentation of the synthesis gas using aspen plus. Chem Eng Trans 2014;37:637–42. https://doi.org/10.3303/CET1437107.
[14] Pardo-Planas O, Atiyeh HK, Phillips JR, Aichele CP, Mohammad S. Process simulation of ethanol production from biomass gasification and syngas fermentation. Bioresour Technol 2017;245:925–32. https://doi.org/10.1016/j.biortech.2017.08.193.
[15] de Medeiros EM, Posada JA, Noorman H, Osseweijer P, Filho RM. Hydrous bioethanol production from sugarcane bagasse via energy self-sufficient gasification-fermentation hybrid route: simulation and financial analysis. J Clean Prod 2017;168:1625–35. https://doi.org/10.1016/j.jclepro.2017.01.165.
[16] de Medeiros EM, Noorman H, Maciel Filho R, Posada JA. Production of ethanol fuel via syngas fermentation: optimization of economic performance and energy efficiency. Chem Eng Sci X 2020;5:100056. https://doi.org/10.1016/j.cesx.2020.100056.
[17] Safarian S, Unnthorsson R, Richter C. Bioethanol production via herbaceous and agricultural biomass gasification integrated with syngas fermentation. Fermentation 2021;7. https://doi.org/10.3390/fermentation7030139.
[18] Sanderson MA, Reed ORL, Mclaughlin SB, Wullschleger SD, Wolf DD, Hopkins C, et al. Switchgrass as a sustainable bioenergy crop. Plant Breed 1996;56:83–93.
[19] Haydary Juma. Chemical process design and simulation: aspen plus and aspen hysys applications. John Wiley & Sons, Inc.; 2018. https://doi.org/10.1002/9781119311478.
[20] Subotić V, Schluckner C, Stoeckl B, Preininger M, Lawlor V, Pofahl S, et al. Towards practicable methods for carbon removal from Ni-YSZ anodes and restoring the performance of commercial-sized ASC-SOFCs after carbon deposition induced degradation. Energy Convers Manag 2018;178:343–54. https://doi.org/10.1016/j.enconman.2018.10.022.
[21] Milne T a, Evans RJ. Biomass gasifier " tars ": their nature , formation , and conversion. Golden, Colorado. 1998. https://doi.org/10.2172/3726.
[22] Marcantonio V, Bocci E, Ouweltjes JP, Del Zotto L, Monarca D. Evaluation of sorbents for high temperature removal of tars, hydrogen sulphide, hydrogen chloride and ammonia from biomass-derived syngas by using Aspen Plus. Int J Hydrogen Energy 2020;45:6651–62. https://doi.org/10.1016/j.ijhydene.2019.12.142.
[23] Mohammed MAA, Shafizah IN, Salmiaton A, Arifin NA, Hafriz RSRM, Azlina WAKGW, et al. H2-rich and tar-free downstream gasification reaction of efb by using the malaysian dolomite as a secondary catalyst. Catalysts 2021;11:1–10. https://doi.org/10.3390/catal11040447.
[24] Björkman E, Sjöström K. Decomposition of ammonia over dolomite and related compounds. Energy Fuel 1991;5:753–60. https://doi.org/10.1021/ef00029a023.
[25] Hoseinzade L, Adams TA. Techno-economic and environmental analyses of a novel, sustainable process for production of liquid fuels using helium heat transfer. Appl Energy 2019;236:850–66. https://doi.org/10.1016/j.apenergy.2018.12.006.
[26] Hanzon L. Technoeconomic analysis of the Co-production of hydrogen and power in thermochemical-based biorefineries. Colorado School of Mines; 2020.
[27] MERICHEM. Removing. H2S from gas streams. Merichem Co Web Site; 2022. https://www.merichem.com/technology/sulfur-recovery-with-lo-cat/%0A. [Accessed 21 February 2022]. accessed.
[28] Xu D, Tree DR, Lewis RS. The effects of syngas impurities on syngas fermentation to liquid fuels. Biomass Bioenergy 2011;35:2690–6. https://doi.org/10.1016/j.biombioe.2011.03.005.
[29] Chen J, Henson MA. In silico metabolic engineering of Clostridium ljungdahlii for synthesis gas fermentation. Metab Eng 2016;38:389–400. https://doi.org/10.1016/j.ymben.2016.10.002.
[30] Tanner RS, Miller LM, Yang D. Clostridial rRNA homology group I. Int J Syst Bacteriol 1993;43:232–6.
[31] Richter H, Martin ME, Angenent LT. A two-stage continuous fermentation system for conversion of syngas into ethanol. Energies 2013;6:3987–4000. https://doi.org/10.3390/en6083987.
[32] Klasson KT, Ackerson MD, Clausen EC, Gaddy JL. Biological conversion of coal synthesis gas to methane. Am Inst Chem Eng Natl Meet 1985;72:1673–8.
[33] Carmo M, Fritz DL, Mergel J, Stolten D. A comprehensive review on PEM water electrolysis. Int J Hydrogen Energy 2013;38:4901–34. https://doi.org/10.1016/j.ijhydene.2013.01.151.
[34] Nami H, Rizvandi OB, Chatzichristodoulou C, Hendriksen PV, Frandsen HL. Techno-economic analysis of current and emerging electrolysis technologies for green hydrogen production. Energy Convers Manag 2022;269:116162. https://doi.org/10.1016/j.enconman.2022.116162.
[35] Yukesh Kannah R, Kavitha S, Preethi Parthiba Karthikeyan O, Kumar G, Dai-Viet NV, et al. Techno-economic assessment of various hydrogen production methods – a review. Bioresour Technol 2021;319:124175. https://doi.org/10.1016/j.biortech.2020.124175.
[36] Aspen Technology. Aspen Energy Analyzer 2013;1–148.
[37] Turton R, Bailie RC, Whiting WB, Shaeiwitz JA. Analysis, synthesis, and design of chemical processes. Third edit. Pearson Education; 2008.
[38] Aden A, Ruth M, Ibsen K, Jechura J, Neeves K, Sheehan J, et al. Lignocellulosic biomass to ethanol process design and economics utilizing Co-current dilute acid prehydrolysis and enzymatic hydrolysis for corn stover. 2002.

[39] Bergtold Jason, Sailus Marty, editors. Conservation tillage systems in the southeast; 2020.
[40] Pipitone G, Zoppi G, Ansaloni S, Bocchini S, Deorsola FA, Pirone R, et al. Towards the sustainable hydrogen production by catalytic conversion of C-laden biorefinery aqueous streams. Chem Eng J 2019;377:120677. https://doi.org/10.1016/j.cej.2018.12.137.
[41] KPMG. The hydrogen trajectory. https://home.kpmg/xx/en/home/insights/2020/11/the-hydrogen-trajectory.html; 2020 (accessed April 19, 2022).
[42] BRYAN MUNICIPAL UTILITIES. Commercial/industrial metering & rates. 2021 (accessed March 3, 2022), https://www.cityofbryan.net/commercialindustrial-metering-rates/#:~:text=Commercial%2FIndustrial Water Rates (effective 12-20-2021)&text=%243.10 per 100 cubic ft,%244.65 per 100 cubic ft.
[43] No Title nd. https://www.made-in-china.com/. [Accessed 5 February 2022]. accessed.
[44] Baddour FG, Snowden-swan LJ. Catalyst cost model development (CatCost). US Dep Energy Bioenergy Technol Off; 2019.
[45] Zhu Y, Albrecht KO, Elliott DC, Hallen RT, Jones SB. Development of hydrothermal liquefaction and upgrading technologies for lipid-extracted algae conversion to liquid fuels. Algal Res 2013;2:455–64. https://doi.org/10.1016/j.algal.2013.07.003.
[46] Guzmán H, Salomone F, Batuecas E, Tommasi T, Russo N, Bensaid S, et al. How to make sustainable CO2 conversion to Methanol: thermocatalytic versus electrocatalytic technology. Chem Eng J 2021;417. https://doi.org/10.1016/j.cej.2020.127973.
[47] Salomone F, Giglio E, Ferrero D, Santarelli M, Pirone R, Bensaid S. Techno-economic modelling of a Power-to-Gas system based on SOEC electrolysis and CO2 methanation in a RES-based electric grid. Chem Eng J 2019;377:120233. https://doi.org/10.1016/j.cej.2018.10.170.
[48] Short W, Packey D, Holt T. A manual for the economic evaluation of energy efficiency and renewable energy technologies, vol. 95; 1995. Golden.
[49] Phillips SD, Jones SB, Meyer PA, Snowden-Swan LJ. Techno-economic analysis of cellulosic ethanol conversion to fuel and chemicals. Biofuels, Bioprod Biorefin 2022. https://doi.org/10.1002/bbb.2346.
[50] Magazine Ethanol producer. U.S. Ethanol Plants n.d. http://www.ethanolproducer.com/plants/listplants/US/Operational/All/page:1/sort:capacity/direction:desc. [Accessed 16 February 2022]. accessed.
[51] Sadhukhan J, Ng KS, Hernandez EM. Biorefineries and chemical processes: design, integration and sustainability analysis, vol. 9781119990; 2014. https://doi.org/10.1002/9781118698129.
[52] Oliveira L, Rückel A, Nordgauer L, Schlumprecht P, Hutter E, Weuster-Botz D. Comparison of syngas-fermenting clostridia in stirred-tank bioreactors and the effects of varying syngas impurities. Microorganisms 2022;10:681. https://doi.org/10.3390/microorganisms10040681.
[53] Ciliberti C, Biundo A, Albergo R, Agrimi G, Braccio G, de Bari I, et al. Syngas derived from lignocellulosic biomass gasification as an alternative resource for innovative bioprocesses. Processes 2020;8:1–38. https://doi.org/10.3390/pr8121567.
[54] Voegele E. Aemetis provide updates of RNG, cellulosic ethanol projects. BIOMASS Mag; 2013. http://biomassmagazine.com/articles/16886/aemetis-provide-updates-of-rng-cellulosic-ethanol-projects. [Accessed 3 May 2022]. accessed.